numbers of PO_4^{3-} ions in an iron oxyhydroxide crystal may be expected to disrupt the regularity of the lattice due to the larger dimensions of the PO_4^{3-} ion relative to O^{2-} and OH^- ions. However, the phosphate content in these materials is of relative proportions high enough for the compounds to be described as hydrated ferric phosphates, and thus they have the potential for a different lattice structure. This indicates that some other mechanism besides the ionic dimensions of PO_4^{3-} may be responsible for their disordered structure.

The two invertebrate proteins in the present study have extremely low inorganic phosphate contents, and yet the electron diffraction indicates only limited crystallinity compared to the cores of human thalassemic spleen[23] and horse spleen ferritins.[8,36,37] These latter ferritins have higher levels of phosphate associated with their cores, although not the very high levels found in the bacterioferritins. It appears, therefore, that for cores with lower levels of phosphate there is not a direct correlation between phosphate content and crystallinity. It is only at higher levels of phosphate that noncrystallinity is ensured. Other factors that determine core structure include the molecular nature of the inner surface of the protein shell, which may influence the rate of Fe(II) oxidation, nucleation and growth of the core,[28] and the rate of ion diffusion and incorporation into the core. Slower rates would give a more crystalline core. The rate of formation of the core may be related to the turnover of iron in the organism. Limpets and chitons have a high turnover of iron necessitated by the need to continuously form iron minerals for structural components of their radulas.[4,5] This could explain the limited crystallinity found in these ferritins and the ferritin of *P. vulgata*.[23]

A further consideration that may account for the weak dependence of the magnetic ordering temperature on phosphate content at low to medium phosphate levels concerns the structural localization of phosphate in the ferritin cores. It is probably only when the phosphate is bound within the core structure that magnetic exchange interactions are diminished, so affecting the magnetic ordering temperature. Weak adsorption of phosphate to the surface sites of the ferrihydrite cores is suggested by the observation that about 77% of the phosphate of horse spleen ferritin cores is lost during alkali treatment,[9] which removes the protein shells from the cores. Furthermore, the P:Fe ratio is rather higher than average in cores with low iron content and lower than average in cores of high iron content,[38] again suggesting surface adsorption of phosphate. Such weak absorption would have minimal influence on both the crystallographic order and the magnetic ordering temperature.

Furthermore, as shown by the lower redox potential required for the reductive dissolution of bacterioferritin cores of *P. aeruginosa* compared with mammalian ferritin,[39] ferritin cores free of phosphate will have increased solubility over those containing phosphate as an integral component of the bulk structure.

This enhanced solubility may be of functional significance in the requirement for rapid iron mobilization and mineralization within the radula tissue. Ferritin from the chiton *A. hirtosa* is known to take up iron very much more rapidly than horse spleen ferritin,[4] and this reactivity is thus consistent with the structural features of the core reported here.

Registry No. Fe, 7439-89-6; PO_4, 14265-44-2; ferrihydrite, 39473-89-7.

(33) Ofer, S.; Papaefthymiou, G. C.; Frankel, R. B.; Lowenstam, H. A. *Biochim. Biophys. Acta* **1981**, *676*, 199.
(34) Kuterbach, D. A.; Walcott, B.; Reeder, R. J.; Frankel, R. B. *Science* **1982**, *218*, 695.
(35) Kuterbach, D. A.; Walcott, B. *J. Exp. Biol.* **1986**, *126*, 375.
(36) Massover, W. H.; Cowley, J. M. *Proc. Natl. Acad. Sci. U.S.A.* **1973**, *70*, 3847.
(37) Harrison, P. M.; Fischbach, F. A.; Hoy, T. G.; Haggis, G. H. *Nature* **1967**, *216*, 1188.
(38) Fischbach, F. A.; Harrison, P. M.; Hoy, T. G. *J. Mol. Biol.* **1969**, *39*, 235.
(39) Watt, G. D.; Frankel, R. B.; Papefthymiou, G. C. *Proc. Natl. Acad. Sci. U.S.A.* **1985**, *82*, 3640.

Contribution from the Department of Chemistry, University of Florence, Via Gino Capponi 7, 50121 Florence, Italy, and Institute of Agricultural Chemistry, University of Bologna, Viale Berti Pichat 10, 40127 Bologna, Italy

^{1}H NMR Studies of the Oxidized and Partially Reduced 2(4Fe-4S) Ferredoxin from *Clostridium pasteurianum* §

Ivano Bertini,*,† Fabrizio Briganti,† Claudio Luchinat,‡ and Andrea Scozzafava†

Received April 19, 1989

^{1}H NMR spectra of the oxidized ferredoxin from *Clostridium pasteurianum*, which contains two weakly paramagnetic $Fe_4S_4^{2-}$ clusters, have been recorded and ^{1}H nuclear Overhauser effects have been used to determine proton pairs of β-CH_2 of the cluster-coordinated cysteines. The shift dependence on the dihedral angles between the Fe-S-C and S-C-H planes has been discussed. The size of the hyperfine shifts and their temperature dependence can be reproduced with a model in which some of the antiferromagnetic coupling constants between Fe(III) and Fe(II) ions are smaller than the other antiferromagnetic coupling constants. ^{1}H saturation transfer experiments on the partially reduced protein provides an estimate of the lower limit of the intermolecular electron transfer between the fully oxidized, intermediate, and fully reduced species.

Introduction

During the last years iron-sulfur proteins have attracted the interest of researchers owing to their role in electron-transfer processes during mitochondrial respiration, nitrogen fixation, and photosynthesis.[1-4] These systems are able to reversibly transfer one or more electrons, undergoing changes in NMR,[5,6] EPR,[7,8] Mössbauer,[7] magnetic susceptibility, and optical properties.[8,9] At least one of the oxidation states of all the known Fe-S proteins

† University of Florence.
‡ University of Bologna.
∥ Abbreviations: *C.p.*, *Clostridium pasteurianum*; DEAE-, (diethylamino)ethyl-; EPR, electron paramagnetic resonance, Fd, ferredoxin; MODEFT, modified driven equilibrium Fourier transform; NMR, nuclear magnetic resonance; NOE, nuclear Overhauser effect; P_i, phosphate; ppm, parts per million; WEFT, water-eliminated Fourier transform.

(1) Hall, D. O.; Evans, M. C. W. *Nature* **1969**, *223*, 1342.
(2) Handford, P. M.; Lee, W. K. In *Inorganic Biochemistry*; The Royal Society of Chemistry: London, 1979; Vol. 2, Chapter 3.
(3) Cammack, R. In *Iron-Sulfur Protein Research*; Matsubara, H., Katsube, Y., Wada, K., Eds.; Japan Scientific Societies Press/Springer Verlag: Berlin, 1987; p. 40.
(4) Evans, M. C. W. In *Iron-Sulfur Proteins*; Spiro, T. G., Ed.; Wiley, New York, 1982; Chapter 6.
(5) Ho, C.; Fung, L. W.-M.; Wiechelman, K. J. *Methods Enzymol.* **1978**, *54*, 192.
(6) Phillips, W. D. In *NMR of Paramagnetic Molecules, Principles and Applications*; La Mar, G. N., Horrocks, W. DeW., Jr., Holm, R. H., Eds.; Academic Press: New York, 1973; Chapter 11.

0020-1669/90/1329-1874$02.50/0

is paramagnetic; the presence of a paramagnetic center makes them quite suitable for NMR spectroscopy and other techniques that monitor changes in the magnetic properties of the protein.[10] Furthermore, the large variability of redox potentials (−400 to +350 mV) among ferredoxins containing the same Fe–S clusters opened questions on the relationship between the structure and the functional properties of this class of proteins.[11]

In all the Fe–S proteins, the antiferromagnetically coupled iron atoms are coordinated to cysteine residues.[12] The β-CH_2 protons of the cysteines are consequently affected by hyperfine interactions with the iron ions. Among the Fe–S proteins, the 8Fe-8S ferredoxin from *Clostridium pasteurianum*, which contains two 4Fe-4S clusters in a cubane structure, is representative of the low-potential bacterial ferredoxins;[12,13] its molecular weight is about 6000, and the single polypeptide chain consists of 55 amino acid residues. The ^{1}H NMR spectrum of *C.p.* ferredoxin shows a substantial number of resonances that are isotropically shifted from the diamagnetic region.[14] Their assignment is important in order to monitor the magnetic properties of the protein and its interactions with redox partners. The assignment of the most downfield shifted resonances in the ^{1}H NMR spectrum of 8Fe-8S ferredoxin to β-CH_2 cysteinyl protons was partially performed by Packer et al. on an analogous ferredoxin from *Clostridium acidi urici*.[15] In the present investigation, we report a detailed analysis of the ^{1}H NMR spectra of *C.p.* ferredoxin in the oxidized and partially reduced states. Super WEFT and MODEFT pulse sequences allowed us to monitor the β-CH_2 protons of cluster bound cysteines. After La Mar et al. had first observed ^{1}H NOE's between geminal protons of cysteines bound to Fe_2S_2 proteins,[16] we pursued the exploitation of ^{1}H nuclear Overhauser enhancement experiments in order to assign vicinal proton pairs. We also demonstrated that saturation transfer experiments allow the correlation among the resonances corresponding to a β-CH_2 proton in the fully oxidized, fully reduced, and intermediate redox states.

Materials and Methods

All chemicals used throughout were of the best quality available. Lyophilized oxidized *C. pasteurianum* ferredoxin was obtained from Sigma Chemical Co., Milwaukee WI, and subjected to further purification. All the columns, flasks, and buffers were flushed with nitrogen or argon. The protein was dissolved in 50 mM NaP_i buffer, pH 8.0, and applied to a DEAE-cellulose column (10 × 50 mm) equilibrated with the same buffer. The ferredoxin was eluted with a 0–0.5 M NaCl linear gradient in 50 mM NaP_i pH 8.0; the fractions with an absorbance ratio A_{390}/A_{280} greater than 0.79 were pooled, concentrated, desalted, and applied to a G-75 Sephadex gel filtration column (10 × 500 mm) equilibrated and run with 50 mM NaP_i, pH 8.0. The fractions with $A_{390}/A_{280} \geq 0.81$ were pooled and concentrated. Experiments in D_2O (99.95%) containing 50 mM NaPi, pH 8.0, were performed by solvent exchange utilizing an ultrafiltration Amicon cell equipped with a YM5 membrane; at least five changes of deuterated buffer were performed to assure satisfactory solvent exchange. The protein samples (1–4 mM) were reduced by addition of small amounts of 0.1 M sodium dithionite in 50 mM NaP_i, 99.9% D_2O, pH 8.0; the extent of reduction was monitored by measuring the area of the NMR peaks corresponding to the various redox species. The pH values are reported as uncorrected pH-meter readings.

High-resolution Fourier transform ^{1}H NMR measurements were carried out on a Bruker CXP 300, a Bruker MSL 200, or a Varian VXR 400 spectrometer running at 300, 200, or 400 MHz, respectively. Typically 1000–5000 transients were acquired by utilizing the MODEFT (90-τ-180-τ-90-AQ) or Super WEFT (180-τ-90-AQ) pulse sequences.[17,18]

^{1}H NOE and saturation-transfer measurements were performed by collecting 2–8K data points over 15–50-KHz bandwidths, respectively. The water signal was suppressed by using the super WEFT pulse sequence with recycle times of 60–90 ms and delay times τ of 50–85 ms. The resonances under investigation were saturated by utilizing a selective decoupling pulse of 0.01–0.02 W kept on for $^9/_{10}$ of the delay time τ. Difference spectra were collected directly by applying the decoupler frequency alternatively according to the scheme

$$\omega_2-(\omega_2 + \delta)-\omega_2-(\omega_2 - \delta)$$

where ω_2 is the frequency of the irradiated signal and δ the off-resonance offset; the receiver phase was alternated accordingly. This sequence scheme allows the obtainement of good difference spectra, minimizing the hardware instabilities. Each experiment, run in block-averaging mode, consisted usually of 30–50 blocks of 16 000 scans each. Exponential multiplication of the free induction decay improved the signal to noise ratio, introducing 5–30 Hz additional line broadening.

T_1 measurements were performed by utilizing either the MODEFT or inversion recovery sequences.[17,19]

Considerations on the Nuclear Overhauser Effect and Saturation Transfer

The nuclear Overhauser effect is defined as the fractional intensity change of a NMR resonance i upon saturation of another resonance j in the same molecular species. The time dependence of the buildup of the NOE for an isolated two spin system is described by eq 1,[20] where ρ_i is the intrinsic relaxation spin–lattice

$$\eta_{ij} = \frac{\sigma_{ij}(1 - e^{-\rho_i t})}{\rho_i} \quad (1)$$

rate for the nucleus i and σ_{ij} is the cross relaxation rate between i and j. In the high-field case ($\omega^2\tau_c^2 \gg 1$), as in the present system at 200–400 MHz, the cross-relaxation rate is given by eq 2, where,

$$\sigma_{ij} = \frac{-\hbar^2\gamma^4\tau_c}{10r_{ij}^6} \quad (2)$$

if local motions are not present, τ_c is the protein tumbling time, and r_{ij} is the internuclear distance. For long irradiation times ($t \gg \rho_i^{-1}$), the steady-state is reached and η_{ij} takes the form

$$\eta_{ij} = \sigma_{ij}/\rho_i \quad (3)$$

NOE measurements of paramagnetic systems are relatively rare because the large intrinsic longitudinal relaxation rates ρ_i make η_{ij} small. However, the paramagnetism undermines spin diffusion, allowing the selective detection of primary NOEs in large proteins. In particular, La Mar et al. have pioneered the exploration of this technique.[21] In the present system, the ρ_i values of the isotropically shifted resonances are between 200 and 40 s^{-1}; for a τ_r value of 2×10^{-9} s, as calculated from the Stokes–Einstein equation for isotropic rotational motion of a MW 6000 protein, and interproton distances of 1.6–1.7 Å, as estimated for β-CH_2 geminal protons, η_{ij} values between 17% and 2.4% are expected.

Signals belonging to the same nuclear species that interconvert among different chemical environments on a time scale comparable with the intrinsic relaxation times may lead through magnetization transfer experiments to establish connectivities among resonances

(7) Munck, E.; Huynh, B. H. In *ESR and NMR of Paramagnetic Species in Biological and Related Systems*; Bertini, I., Drago, R. S., Eds.; D. Reidel Publishing Co.: Dordrecht, The Netherlands, 1979; Chapter 12.
(8) Hall, D. O. In *Bioinorganic Chemistry*, Raymond, K. N., Ed.; Advances in Chemistry 162; American Chemical Society; Washington, DC, 1977; Vol. 2, Chapter 13.
(9) Orme-Johnson, W. H. In *Inorganic Biochemistry*, Eichhorn, G. L., Ed., Elsevier: Amsterdam, 1973; Vol. 2, Chapter 22.
(10) Bertini, I.; Luchinat, C. *NMR of Paramagnetic Molecules in Biological Systems*; Benjamin/Cummings: Menlo Park, CA, 1986.
(11) Adman, E.; Watenpaugh, K. D.; Jensen, L. H. *Proc. Natl. Acad. Sci. U.S.A.* **1975**, *72*, 4854.
(12) Bezkorovainy, A. *Biochemistry of Nonheme Iron*; Plenum Press: New York, 1980; Chapter 8.
(13) Rabinowitz, J. C. In *Bioinorganic Chemistry*; Dessy, R., Dillard, J., Taylor, L., Eds.; Advances in Chemistry 100; American Chemical Society: Washington, DC, 1971; Chapter 15.
(14) Poe, M.; Phillips, W. D.; McDonald, C. C.; Lovenberg, W. *Proc. Natl. Acad. Sci. U.S.A.* **1970**, *65*, 797.
(15) Packer, E. L.; Sweeny, W. V.; Rabinowitz, J. C.; Sternlicht, H.; Shaw, E. N. *J. Biol. Chem.* **1977**, *252*, 2245.
(16) La Mar, G. N.; Dugad, L. B.; Banci, L.; Bertini, I. *Biochemistry*, in press.
(17) Hochmann, J.; Kellerhals, H. *J. Magn. Reson.* **1980**, *38*, 23.
(18) Inubushi, T.; Becker, E. D. *J. Magn. Reson.* **1983**, *51*, 128.
(19) Vold, R. L.; Waugh, J. S.; Klein, M. P.; Phelps, D. E. *J. Chem. Phys.* **1968**, *48*, 3831.
(20) Noggle, J. H.; Shirmer, R. E. *The Nuclear Overhauser Effect*; Academic: New York, 1971.
(21) Thanabal, V.; de Ropp, J. S.; La Mar, G. N. *J. Am. Chem. Soc.* **1987**, *109*, 265.

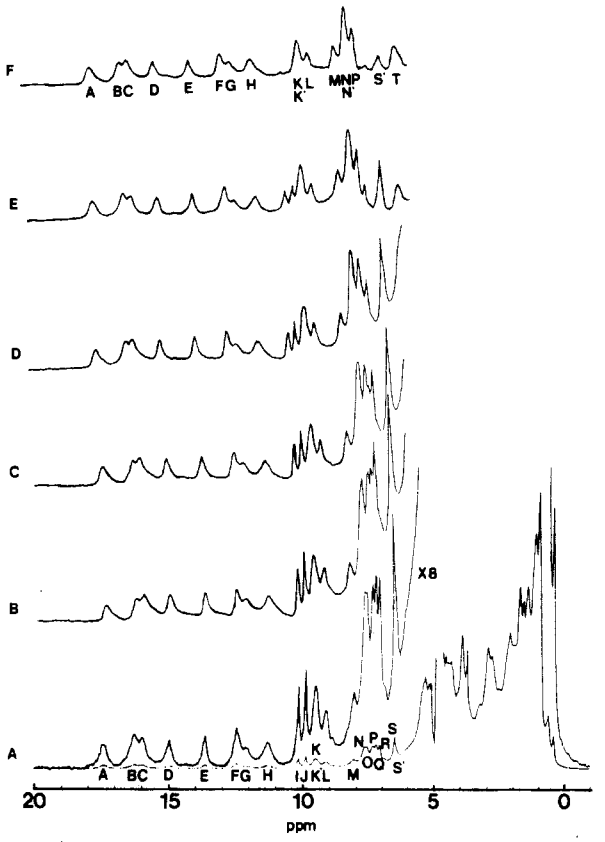

Figure 1. ^{1}H NMR spectra of oxidized *C. pasteurianum* ferredoxin in D_2O, pH 8.0, at 298 K: (A) reference spectrum at 300 MHz; (B–F) spectra obtained by using the super WEFT pulse sequence at different times τ of 150 (B), 80 (C), 60 (D), 40 (E), and 30 (F) ms, respectively.

and to extend known assignments in one chemical environment to the other environments in equilibrium with the former. In the case of two species in equilibrium A $\rightleftharpoons$ B, by presaturation of the B resonance a decrease in intensity of the A resonance is obtained. This may be related to the time of exchange from A, τ_A, through eq 4,[22,23] where M_z and M_0 are the magnetizations observed with

$$\tau_A = T_1^A \frac{M_z^A/M_0^A - M_z^B/M_0^B}{1 - M_z^A/M_0^A} \quad (4)$$

and without irradiation of signal B and T_1^A is the intrinsic spin–lattice relaxation time for the nucleus in the A environment in the absence of exchange.

Results and Discussion

The ^{1}H NMR spectrum of the oxidized *C.p.* Fd in 50 mM NaP_i, pH 8.0, in 99.95% D_2O recorded at 200 MHz and 25 °C is shown in Figure 1A. This ferredoxin exhibits relatively well-resolved resonances in the diamagnetic region from −2 to +8 ppm, and in addition a series of 14 isotropically shifted resonances (A–M) in the 8–18 ppm region. The *C.p.* ferredoxin contains two 4Fe-4S clusters coordinated to the protein through Fe–cysteinyl sulfur bonds; in the oxidized form, they display a diamagnetic ground state arising from antiferromagnetic exchange coupling of the iron ions as suggested also by magnetic susceptibility measurements.[14] The excited levels are thermally accessible and account for the magnetic susceptibility. Proton NMR studies of model compounds have shown that the proton shifts are mainly contact in origin;[24] therefore, the 16 β-CH_2 protons of the iron-coordinated cysteines are expected to be isotropically shifted. Isotopic labeling experiments performed on an analogous ferredoxin from *C. acidi urici* have shown that the eight resonances above 10 ppm are all β-CH_2 protons,[15] whereas in the region below 10 ppm complex envelopes contain other α-CH and β-CH_2 signals. The T_1 values of the isotropically shifted resonances of the oxidized ferredoxins are reported in Table I. The eight resonances above 10 ppm show the shortest relaxation times, between 4.4 and 13.1 ms, in agreement with the closest distance of the β-CH_2 protons to the paramagnetic centers. Beyond its common use as water-suppressing pulse sequences, the Super WEFT and the MODEFT sequences can be utilized with different delay times to detect fast relaxing resonances hidden in the diamagnetic region. In Figure 1B–F the spectra recorded with the super WEFT pulse sequence with delay times of 150, 80, 60, 45, and 30 ms are reported. It is evident that in the region below 10 ppm many resonances disappear as the delay time is decreased to 30 ms. These spectra show the presence of eight to nine fast relaxing resonances ($T_1 \leq 20$ ms) in the diamagnetic region from 10 to 5 ppm. Analogous results are obtained by using the MODEFT pulse sequence. The resonances A–H, K–N′, P, S′, and T are therefore assigned to protons in the immediate surroundings of the paramagnetic 4Fe-4S clusters. This is also confirmed from the temperature dependence of the shifts (Figure 2) since the isotropic shifts are temperature dependent.[14] As the temperature is increased all the resonances detected with the super WEFT sequence by using short τ delays are shifted to lower field; this anti-Curie behavior is explained by considering an antiferromagnetic exchange coupling among the iron atoms of each cluster; the increase in temperature allows the higher energy levels to increase their population, increasing the magnetic susceptibility of the system.[14] The T_1 values of these isotropically shifted resonances, as estimated from inversion recovery and super WEFT pulse sequences, range from 4.4 to ≅20

Table I. 200-MHz ^{1}H NMR Shift and T_1 Values at 298 K for the Isotropically Shifted Signals in the Oxidized *C. pasteurianum* Ferredoxin

signal	δ, ppm	T_1,[a] ms	assignt[b]
A	17.3	7.0	β-CH_2 (1)
B	16.2	9.3	β-CH_2 (2)
C	16.0	8.1	β-CH_2 (3)
D	14.9	10.7	β-CH_2 (4)
E	13.6	13.1	β-CH_2
F	12.5	10.7	β-CH_2
G	12.2	6.0	β-CH_2 (5)
H	11.2	4.4	β-CH_2 (6)
I	10.1	30.3	α-CH
J	9.9	30.2	α-CH
K	9.6	14.5	β-CH_2 (1)
K′	9.6	14.5	β-CH_2 (3)
L	9.1	16.8	β-CH_2 (5)
M	8.15	11.8	β-CH_2 (6)
N	7.7	16.2	β-CH_2 (2)
N′	7.7	16.2	
P	7.5	15–20[c]	
S′	6.5	15–20[c]	β-CH_2 (4)
T	5.8	15–20[c]	

[a] Estimated errors are within ±10%. [b] The numbers in parentheses indicate the pairs of β-CH_2 protons as assigned through nuclear Overhauser effects measurements. [c] Estimated from the super WEFT spectra at different delay times τ.

Table II. Observed Nuclear Overhauser Effects[a] between Isotropically Shifted Signals in the Oxidized *C. Pasteurianum* Ferredoxin

obsd peaks						satd peaks
K	K′	L	M	N	S′	
5.1						A
				7.4		B
	5.6					C
					6.5	D
		6.1				G
			5.7			H

[a] The data were recorded at 300 or 200 MHz and 25 °C and are reported as percent decrease in signal intensity.

(22) Sandstrom, J. *Dynamic NMR Spectroscopy*; Academic: New York, 1982; Chapter 4.
(23) Gupta, R. K.; Redfield, A. G. *Biochem. Biophys. Res. Commun.* **1970**, *41*, 273.
(24) Averill, B. A.; Orme-Johnson, W. H. In *Metal Ions in Biological Systems*; Sigel, H., Ed., 1978; Vol. 7, Chapter 4.

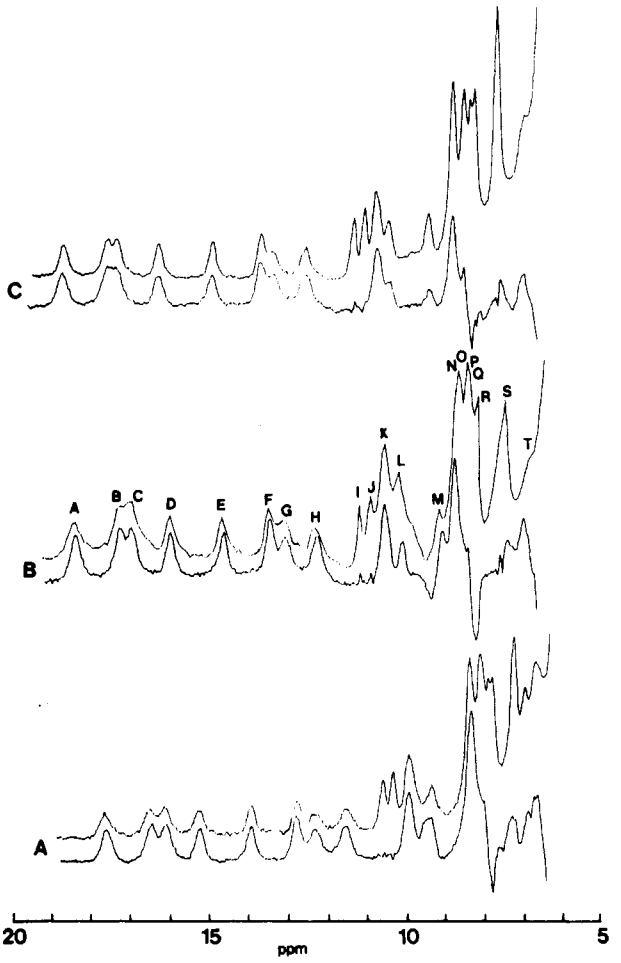

Figure 2. ^{1}H NMR spectra of oxidized *C. pasteurianum* ferredoxin in D_2O, pH 8.0. All the spectra were recorded at 300 MHz, utilizing the super WEFT sequence with delay times τ of 150 (upper spectra) and 35 ms (lower spectra) at 278 (A), 298 (B), and 318 (C) K.

ms (Table I). The signals with T_1 values of about 30 ms (signals I and J) are assigned to cysteinyl α-CH protons.

We performed ^{1}H NOE experiments to assign the pairs of geminal β-CH_2 protons of the cysteines coordinated to the Fe–S clusters. The difference spectra obtained upon saturation of some of the resonances above 10 ppm are reported in Figures 3 and 4. Saturation of A–D, G, and H induces NOEs greater than 5% to peaks K, N, K′, S′, L, and M respectively, while saturation of peaks E and F does not show any NOE above 1.5%. All the NOE values are reported in Table II: the calculated distances are consistent with geminal protons (1.6–1.8 Å), assuming for τ_c a value of 2×10^{-9} s, as obtained from the Stokes–Einstein relationship. The reason why saturation of E and F does not show NOEs comparable to the other pairs is not clear. A possible explanation could be that the corresponding geminal protons may have quite short T_1 or τ_c, too short to allow the detection of NOE greater than 1.5%. Signals E and F may be due to protons not belonging to cysteinyl β-CH_2; however, isotope labeling of the analogous *C. acidi urici* Fd suggests that they indeed are β-CH_2 protons.[15]

The presence of more than 4 NOEs indicates that the two clusters have a similar magnetic behavior, and the assignment of the pairs of β-CH_2 protons points out that the spreading of these signals is comparatively large. The isotropic contact hyperfine coupling between axial and equatorial geminal protons bound to the metal coordinated sulfurs are expected to depend on the dihedral angle ϕ between the H–C–S and the C–S–Fe planes in the iron-coordinated cysteines according to eq 5,[26-28] where B_2

$$A = \beta_0 + B_2 \cos^2 \phi \qquad (5)$$

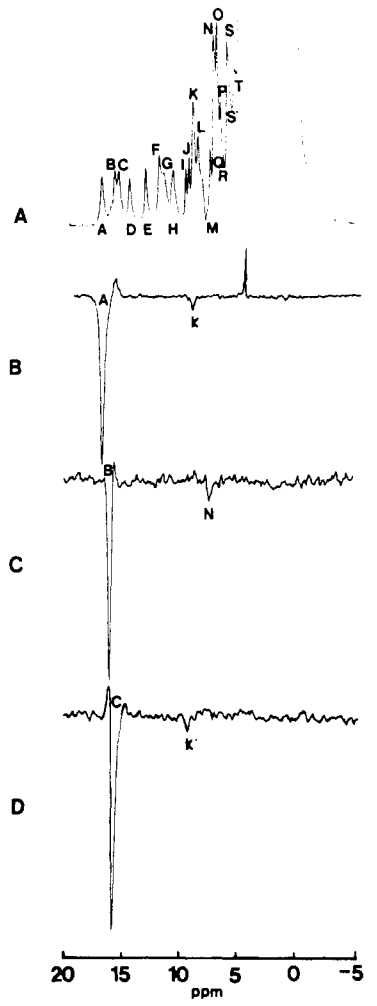

Figure 3. ^{1}H NMR spectra of oxidized *C. pasteurianum* ferredoxin in D_2O, pH 8.0, at 298 K: (A) reference spectrum at 300 MHz; (B–D) steady-state NOE difference spectra obtained by saturating peaks A, B, and C, respectively. All the spectra were recorded at 300 MHz except for spectrum B, which was recorded at 200 MHz.

$\cos^2 \phi$ is related to the spin density on the proton resulting from hyperconjugation and β_0 is related to spin density resulting from other delocalization mechanisms. Spin density transferred to a nonbonding p orbital of the cysteinyl sulfur atoms is sensed by the β-CH_2 protons through hyperconjugative mechanisms. These processes, well characterized in carbon- and nitrogen-based compounds,[28] should be similar in species where sulfur is involved. The values of the dihedral angles ϕ obtained by computer graphics analyses of the X-ray structure at 2.0-Å resolution of the 2-(4Fe-4S) ferredoxin from *Peptococcus aerogenes*, which has a 70% homology with *C. pasterianum* Fd,[25] were used to analyze the spreading of the signals. *P. aerogenes* Fd shares with *C.p.* the essential feature of having 8 of the 16 expected β-CH_2 signals in the downfield region well outside the diamagnetic envelope.[15] Therefore, it is reasonable to assume that the remaining β-CH_2 signals are buried in the diamagnetic region as in the present case. Figure 5A shows the pattern of the shifts for the 16 β-CH_2 signals calculated from eq 5 and the structural data of *P. aerogenes* Fd. The calculation was performed by using a diamagnetic value for the shifts of the β-CH_2 protons of 3.0 ppm, $\beta_0 = 0$, and a B_2 value (11.5 ppm) choosen arbitrarily to visually help in comparing the calculated spectrum with the experimental spectrum of *C.p.* Fd. A scheme of the latter spectrum is reported in Figure 5B for comparison. It can be noted that there is no expected NOE between the eight most downfield shifted signals: each of them is expected to give NOE with less shifted signals as in the present

(25) Adman, E. T.; Sieker, L. C.; Jensen, L. H. *J. Biol. Chem.* **1976**, *251*, 3801.

(26) Heller, C.; McConnell, H. M. *J. Chem. Phys.* **1960**, *32*, 1575.
(27) Ho, F. F.-L.; Reilley, C. N. *Anal. Chem.* **1969**, *41*, 1835.
(28) Stone, E. W.; Maki, A. H. *J. Chem. Phys.* **1962**, *37*, 1326.

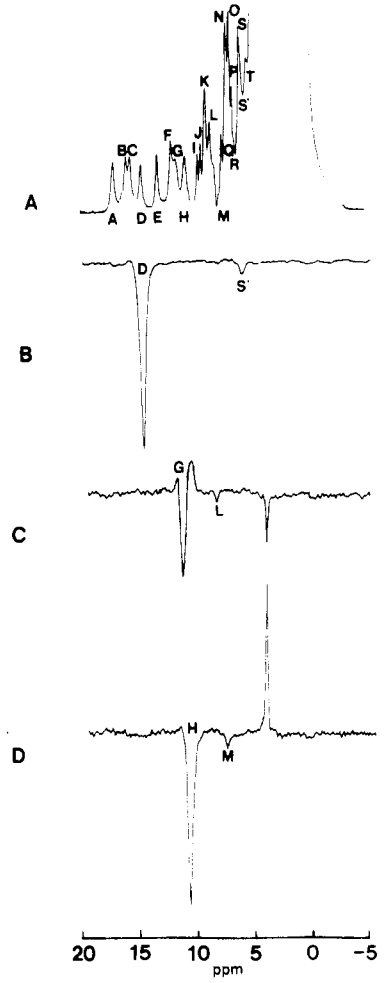

Figure 4. ^{1}H NMR spectra of oxidized *C. pasteurianum* ferredoxin in D_2O, pH 8.0, at 298 K: (A) reference spectrum at 300 MHz; (B–D) steady-state NOE difference spectra obtained by saturating peaks D, G, and H, respectively. All the spectra were recorded at 300 MHz except for spectrum D, which was recorded at 200 MHz.

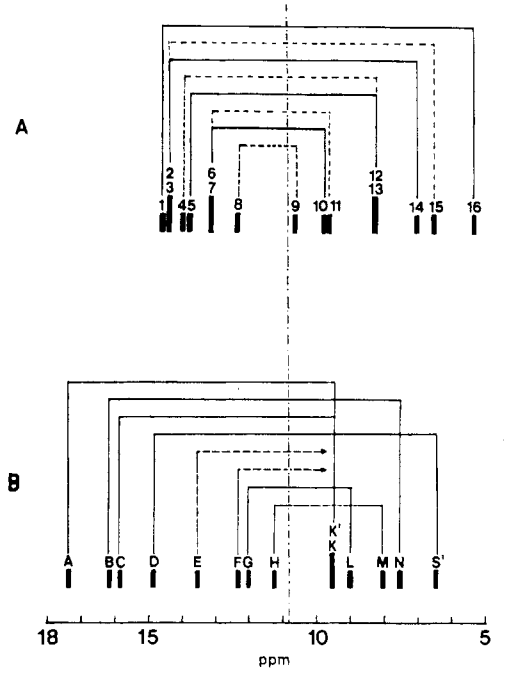

Figure 5. (A) β-CH_2 cysteinyl proton shift pattern calculated from eq 5 and X-ray structural data of *P. aerogenes* Fd as reported in the Results and Discussion; lines connect proton shifts belonging to the same β-CH_2 ((—) cluster I; (- - -) cluster II). (B) Scheme of the experimental spectrum of β-CH_2 cysteinyl protons of *C.p.* Fd at pH 8.0 and 298 K. The lines link resonances that are connected by NOE measurements. No experimental connection is observed for signals E and F. The vertical line is a visual help to separate signals 1–8 and A–H from the others in the calculated and experimental spectra, respectively.

Scheme I

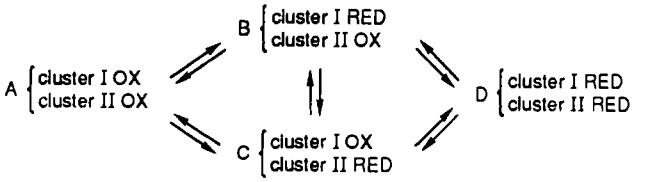

experiment. Therefore, the comparison confirms the overall pattern of the shifts assigned to the β-CH_2 cysteinyl protons. Computer graphics analysis of the *P. aerogenes* Fd shows that there are no protons close to the clusters, and therefore no other nonexchangeable protons can experience a large isotropic interaction except the cysteinyl protons. A comment is due to the fact that the β-CH_2 protons with resonances below 10 ppm have longer T_1 times than those with resonances above 10 ppm. In the present assignment, one of the former set and one of the latter set are due pairwise to geminal protons of the same β-CH_2 group. The protons with smaller shifts are generally closer to the paramagnetic center and should have smaller T_1 values; it is possible that the present results are due to contributions from fractions of unpaired electrons delocalized on the sulfur. This would be the same unpaired spin density originating the contact shifts.

As already reported, spectra of 2(4Fe-4S) ferredoxins in intermediate reduction states display a series of resonances in addition to those of the completely reduced and oxidized proteins (Figure 6).[29,30] They are attributable to species B and C (Scheme I) in which one cluster is oxidized and the other one is reduced. On the NMR time scale the intramolecular electron transfer between the two clusters, about 12 Å apart, is fast and generates a single set of new resonances whose shifts are a weighted average between those of the corresponding oxidized and reduced species. Polarographic studies pointed out that the two clusters have about the same potential, ≈−400 mV, the difference being smaller than the experimental error (≤10 mV).[31] ^{13}C NMR measurements allowed Packer et al. to distinguish among the signals originated from the aromatic residues close to the clusters and to calculate the difference of the redox potential of the two clusters.[32] Saturation-transfer experiments have been performed on *C.p.* ferredoxin in intermediate reduction states. In Figure 6C the saturation transfer difference spectrum obtained by saturating peak C of the reduced species is reported; magnetization is transferred to peak H of the intermediate species and to peak L of the completely oxidized redox species. An analogous pattern is obtained by saturating peak F of the intermediate form: magnetization transfer to peak E of the completely reduced species and to peak A of the oxidized form is shown in Figure 6D. Peaks A and L of the oxidized form have been assigned to β-CH_2 cysteinyl protons by NOE experiments (Table II) and the saturation-transfer measurements allow us to extend these assignments to the corresponding resonances of the intermediate (F and H peaks) and completely reduced (E and C peaks) redox species. These experiments demonstrate that, under the conditions used, also the interprotein electron transfer is fast on the NMR relaxation time scale (~100% magnetization transfer), and more importantly, such measurements provide connections among the signals of the intermediate species and the corresponding reso-

(29) Phillips, W. D.; Poe, M. In *Iron-Sulfur Proteins*; Lovenberg, W., Ed.; Academic Press: New York, 1977; Vol. 3, Chapter 7.
(30) Gaillard, J.; Moulis, J.-M.; Meyer, J. *Inorg. Chem.* **1987**, *26*, 320.
(31) Hill, C. L.; Renaud, J.; Holm, R. H.; Mortenson, L. E. *J. Am. Chem. Soc.* **1977**, *99*, 2549.
(32) Packer, E. L.; Sternlicht, H.; Lode, E. T.; Rabinowitz, J. T. *J. Biol. Chem.* **1975**, *250*, 2062.

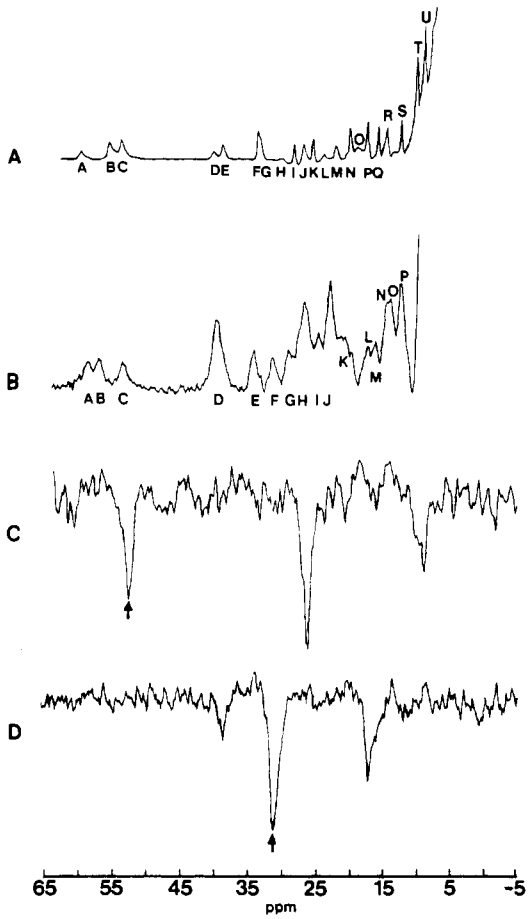

Figure 6. ^{1}H NMR spectra of reduced (A) and partially oxidized (≈ 60%) (B) *C. pasteurianum* ferredoxin in D_2O, pH 8.0. (C and D) Saturation-transfer difference spectra obtained by saturating a peak of the reduced form (C) and one of the intermediated redox species (D), respectively (indicated by arrows). All the spectra were recorded at 200 MHz and 298 K, except that spectrum A was recorded at 400 MHz and 293 K.

nances of the completely reduced and oxidized forms. The calculated lower limit for the electron-transfer rate is $\simeq 6 \times 10^2$ s^{-1}. If the redox potentials of the clusters were the same, we would expect the resonances of the intermediate species to have an averaged shift value between the species in the extreme redox states. This does not happen; in fact, we observe that in Figure 6D the intermediate resonance is more shifted toward the reduced species and in Figure 6C it is more shifted toward the oxidized species. This might imply that the proton giving rise to the three resonances in Figure 6D belongs to a cysteine bound to the cluster with the slightly higher reduction potential whereas the proton giving rise to the three resonances in Figure 6C belongs to a cysteine bound to the other cluster.

Concluding Remarks and Theoretical Considerations

Use of suitable pulse sequences has allowed the revelation of signals of protons feeling the paramagnetic clusters well inside the diamagnetic part of the spectrum. ^{1}H NOEs have been detected for geminal protons owing to their short reciprocal distances, despite the short T_1. This allowed us to assign the pairs of geminal protons, and to try to test eq 5 with respect to the structure of the analogous ferredoxin from *P. aerogenes*. It appears that the spreading of the signals is largely due to differences in isotropic shifts within each β-CH_2 proton pair rather than to intrinsic differences between different pairs. The shifts are smaller with respect to those in the analogous Fe_2S_2 clusters, and all show anticurie behavior.[33]

A consequence of these findings is that, at variance with Fe_2S_2 systems, individual iron sites cannot be distinguished by NMR.[34]

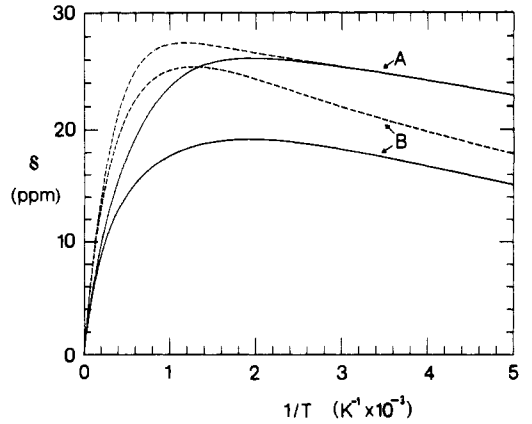

Figure 7. Temperature dependence of the ^{1}H NMR isotropic shifts of oxidized ferredoxin calculated by using eq 6 (A_c/h = 1 MHz). (A) J = 100 cm^{-1} and $\Delta J_{12} = \Delta J_{34}$ = 100 cm^{-1}, with $Fe_1 = Fe_2$ = Fe(II) (—) and $Fe_3 = Fe_4$ = Fe(III) (---). This choice corresponds to J values of 100 cm^{-1} for the four Fe(II)–Fe(III) pairs and 200 cm^{-1} for the Fe(II)–Fe(II) and Fe(III)–Fe(III) pairs (1–2 and 3–4 respectively). (B) J = 200 cm^{-1} and $\Delta J_{12} = \Delta J_{34}$ = −50 cm^{-1}, with $Fe_1 = Fe_3$ = Fe(II) (—) and $Fe_2 = Fe_4$ = Fe(III) (---). This choice corresponds to J values of 150 cm^{-1} for two Fe(II)–Fe(III) pairs (1–2 and 3–4) and 200 cm^{-1} for the other four pairs. If double exchange is present the shifts should be given by some kind of average between the Fe(II) (—) and Fe(III) (---) curves.

The protein has a paramagnetism roughly corresponding to 4 μ_B for each cluster,[14] and the nuclear T_1 values of β-CH_2's are relatively short. They range from 4 to 16 ms. If we consider that T_1 values of β-CH_2's bound to Fe(II) in reduced Fe_2S_2 Fd are slightly shorter (3–8 ms) and that the paramagnetism is slightly larger, we should conclude that the electronic relaxation times in the Fe_4S_4 cluster are of the same order of magnitude as those of Fe_2S_2 systems.[33,34] Again, the difference in T_1 between β-CH_2 protons is mostly due to their axial/equatorial positions than to binding to iron(II) or iron(III).

The impossibility to distinguish between cysteines bound to iron(II) and to iron(III) suggests that the delocalization between iron(II) and iron(III) may be larger than in reduced Fe_2S_2 proteins. The magnetic susceptibility data for a model of Fe_4S_4 cluster were qualitatively reproduced by Holm et al. using J values ranging from 450 to 550 cm^{-1}.[35] We have tried to match the room-temperature susceptibility and isotropic shift data with analytical equations of the type described by Noodleman[36]

$$E = (J/2)[S(S+1)] \pm B_{12}(S_{12} + \tfrac{1}{2}) \pm B_{34}(S_{34} + \tfrac{1}{2}) + (\Delta J_{12}/2)[S_{12}(S_{12}+1)] + (\Delta J_{34}/2)[S_{34}(S_{34}+1)]$$

$$\langle S_{iz}\rangle / \langle S_z\rangle = \alpha_i \gamma_i / \Delta_i \qquad (6)$$

where

$$\alpha_i = [S_{ij}(S_{ij}+1) + S_i(S_i+1) - S_j(S_j+1)]/2$$

$$\gamma_i = [S(S+1) + S_{ij}(S_{ij}+1) - S_{kl}(S_{kl}+1)]/2$$

$$\Delta_i = S_{ij}(S_{ij}+1)S(S+1)$$

and i and j correspond to the iron sites of one pair (1–2 or 3–4), whereas k and l correspond to the iron sites of the other pair. ΔJ_{12} and ΔJ_{34} are the perturbations to J_{12} and J_{34} with respect to the other J values. In the case where the 1–2 and 3–4 pairs are mixed-valence pairs (i.e. they are constituted by one Fe(II) and one Fe(III) ion each), the resonance delocalization parameters B_{12} and B_{34} can be introduced.[36]

Such equations allow therefore the use of different values of J for two out of the six coupling constants. We have learned that

(33) Bertini, I.; Lanini, G.; Luchinat, C. *Inorg. Chem.* **1984**, *23*, 2729.
(34) Banci, L.; Bertini, I.; Luchinat, C. *Structure and Bonding* **1990**, *72*, 113–135.
(35) Papaefthymiou, G. C.; Laskowski, E. J.; Frota-Pessoa, S.; Frankel, R. B.; Holm, R. H. *Inorg. Chem.* **1982**, *21*, 1723–1728.
(36) Noodleman, L. *Inorg. Chem.* **1988**, *27*, 3677–3679.

the magnetic moment of the present system and the anti-Curie temperature dependence around room temperature can be reproduced by J values of 100–200 cm^{-1}. As an example, a set of J values of 100 cm^{-1} for the Fe(II)–Fe(III) pairs and 200 cm^{-1} for the Fe(III)–Fe(III) and Fe(II)–Fe(II) pairs gives a room-temperature μ_{eff} value of $\simeq 3.3\ \mu_B$ and very similar isotropic shifts (calculated by using $A_c/h = 1$ MHz)[34,37] for all cysteines, showing the right order of magnitude (Figure (7A). Similar results are obtained by using a set of J values of 150 cm^{-1} for two of the four possible mixed-valence pairs and 200 cm^{-1} for all the other pairs (Figure 7B). The introduction of double exchange effects[38-40] within the two mixed-valence pairs in the latter case does not yield qualitatively different results. Double exchange is undoubtedly present in these systems since Mössbauer data show mixed-valence behavior for all iron atoms. However, at the present state of knowledge it cannot be established whether double-exchange effects or intrinsic differences in J values are more responsible for the anti-Curie behavior of all the NMR signals.

In the presence of fully reduced, one-electron-oxidized, and fully oxidized species, saturation-transfer experiments are possible, and they allow us to set the lower limit of the electron-transfer rate and provide a tool for the assignment of all the signals of the various species. The limitation of this technique at the present stage is that the spectrum of the semireduced Fd is overcrowded with signals.

Registry No. Cysteine, 52-90-4.

(37) Tsukihara, T.; Fukuyama, K.; Nakamura, M.; Katsube, Y.; Tanaka, N.; Kakudo, M.; Wada, K.; Hase, T.; Matsubara, H. *J. Biochem.* **1981**, *90*, 1763-1773.
(38) Papaefthymiou, V.; Girerd, J. J.; Moura, I.; Moura, J. J. G.; Münck, E. *J. Am. Chem. Soc.* **1987**, *109*, 4703.
(39) Münck, E.; Papaefthymiou, V.; Surerus, K. K.; Girerd, J. J. In *Metals in Proteins*; Que, L., Ed.; ACS Symposium Series; American Chemical Society: Washington, DC, 1988.
(40) Sontum, S. F.; Noodleman, L.; Case, D. A. In *The Challenge of d and f Electrons, Theory and Computation*; Salahub, D. R., Zerner, M. C., Eds.; ACS Symposium Series; American Chemical Society: Washington, DC, 1989.

Contribution from the Department of Chemistry, Gorlaeus Laboratories, Leiden University, P.O. Box 9502, 2300 RA Leiden, The Netherlands

Characterization of Products from [PtCl(dien)]Cl and *S*-Adenosyl-L-homocysteine. Evidence for a pH-Dependent Migration of the Platinum Moiety from the Sulfur Atom to the Amine Group and Vice Versa

Edwin L. M. Lempers and Jan Reedijk*

Received September 6, 1989

The reaction of [PtCl(dien)]Cl with *S*-adenosyl-L-homocysteine (SAH) has been followed by ^1H and ^{195}Pt NMR in the range $2 < pH < 12$. Three products are formed: the mononuclear complex [Pt(dien)SAH-*S*]$^{2+}$ (**1**), with platination of SAH at the sulfur atom, the mononuclear complex [Pt(dien)SAH-*N*]$^{+}$ (**2**), which has a Pt(dien)$^{2+}$ unit coordinated to the amine group of the homocysteine unit, and the dinuclear complex [{Pt(dien)}$_2$SAH-*S*,*N*]$^{3+}$ (**3**), which contains a Pt(dien)$^{2+}$ unit coordinated to the sulfur atom as well as a Pt(dien)$^{2+}$ unit coordinated to the amine group of the cysteine group. No coordination to the adenine unit has been observed under the present conditions. At $pH < 7$ only **1** was formed ($t_{1/2}$ = 75 min for 5 mM concentrations). At $pH > 7$, **1** spontaneously isomerizes to **2** ($t_{1/2}$ = 10 min). This process can be reversed at $pH < 5$ ($t_{1/2}$ = 2 h). At $pH > 7$ the following sequence of reactions occurs between 1 equiv of SAH and 2 equiv of [PtCl(dien)]Cl: SAH → **1** → **2** → **3**. No reaction of SAH directly leading to **2** could be detected. All three complexes react with sodium diethyldithiocarbamate (Na(ddtc)) forming, eventually, free SAH and [Pt(dien)ddtc]$^{+}$. Complexes **2** and **3** both consist of a pair of diastereomers due to different configurations at the sulfur atom. It could be proven for **1** that the interconversion of these isomers was slow on the NMR time scale at 255 K.

Introduction

Platinum–nucleic acid interactions play an important role in the mechanism of action of the antitumor agent *cis*-$PtCl_2(NH_3)_2$ (*cis*-Pt).[1,2] Therefore, research has so far mainly focused on these interactions. Sulfur-containing molecules, like proteins and peptides such as glutathione, are also known to be reactive with Pt ions.[3] It is thought that these constituents of the cytoplasm are responsible for the inactivation of *cis*-Pt and for the observed nephrotoxicity.[4-8] To understand these negative effects, it is necessary to study the chemical reactivity of Pt antitumor drugs with respect to sulfur-containing molecules.

The coordination chemistry of *cis*-Pt and related platinum compounds toward methionine, cysteine, glutathione, and derivatives has already been the subject of some research. Initial binding takes place at the sulfur atom.[9,10] In these initially formed compounds, amine ligands coordinated trans to the sulfur atom become labile.[9-12] Furthermore, with respect to nucleophiles like sodium diethyldithiocarbamate, the Pt–S cysteine bond shows a high degree of stability, whereas the Pt–S methionine bond is thermodynamically labile.[12,13a,b] As a result the formed Pt–S methionine bond is cleaved.

(1) Reedijk, J.; Fichtinger-Schepman, A. M. J.; van Oosterom, A. T.; van de Putte, P. *Struct. Bonding (Berlin)* **1987**, *67*, 53-89.
(2) Sherman, S. E.; Lippard, S. J. *Chem. Rev.* **1987**, *87*, 1153-1181.
(3) Basolo, F.; Pearson, R. G. *Mechanism of Inorganic Reactions*; Wiley: New York, 1967.
(4) Kulamowicz, I.; Olinski, R.; Walter, Z. *Z. Naturforsch., C* **1984**, *39*, 180-182.
(5) Eastman, A. *Chem. Biol. Interact.* **1987**, *61*, 241-248.
(6) Eastman, A.; Barry, M. A. *Biochemistry* **1987**, *26*, 3303-3307.
(7) Micetich, K.; Zwelling, L. A.; Kohn, K. W. *Cancer Res.* **1983**, *43*, 3609-3613.
(8) Borch, R. F.; Pleasants, M. E. *Proc. Natl. Acad. Sci. U.S.A.* **1979**, *76*, 6611-6614.
(9) Appleton, T. G.; Connor, J. W.; Hall, J. R.; Prenzler, P. D. *Inorg. Chem.* **1989**, *28*, 2030-2037.
(10) Appleton, T. G.; Connor, J. W.; Hall, J. R. *Inorg. Chem.* **1988**, *27*, 130-137.
(11) Norman, R. E.; Sadler, P. J. *Inorg. Chem.* **1988**, *27*, 3583-3587.
(12) Lempers, E. L. M.; Reedijk, J. *Inorg. Chem.* **1990**, *29*, 217-222.
(13) (a) Lempers, E. L. M.; Inagaki, K.; Reedijk, J. *Inorg. Chim. Acta* **1988**, *152*, 201-207. (b) Andrews, P. A.; Wung, W. E.; Howell, S. B. *Anal. Biochem.* **1984**, *143*, 46-56.

0020-1669/90/1329-1880$02.50/0